

Journal of Biomedical Optics

SPIEDigitalLibrary.org/jbo

Dual-wavelength photoacoustic technique for monitoring tissue status during thermal treatments

Yi-Sing Hsiao
Xueding Wang
Cheri X. Deng

Dual-wavelength photoacoustic technique for monitoring tissue status during thermal treatments

Yi-Sing Hsiao,^a Xueding Wang,^b and Cheri X. Deng^a

^aUniversity of Michigan, Department of Biomedical Engineering, Ann Arbor, Michigan 48109

^bUniversity of Michigan, Department of Radiology, Ann Arbor, Michigan 48109

Abstract. Photoacoustic (PA) techniques have been exploited for monitoring thermal treatments. However, PA signals depend not only on tissue temperature but also on tissue optical properties which indicate tissue status (e.g., native or coagulated). The changes in temperature and tissue status often occur simultaneously during thermal treatments, so both effects cause changes to PA signals. A new dual-wavelength PA technique to monitor tissue status independent of temperature is performed. By dividing the PA signal intensities obtained at two wavelengths at the same temperature, a ratio, which only depends on tissue optical properties, is obtained. Experiments were performed with two experimental groups, one with untreated tissue samples and the other with high-intensity focused ultrasound treated tissue samples including thermal coagulated lesion, using *ex vivo* porcine myocardium specimens to test the technique. The ratio of PA signal intensities obtained at 700 and 800 nm was constant for both groups from 25 to 43°C, but with distinct values for the two groups. Tissue alteration during thermal treatment was then studied using water bath heating of tissue samples from 35 to 60°C. We found that the ratio stayed constant before it exhibited a marked increase at around 55°C, indicating tissue changes at this temperature. © 2013 Society of Photo-Optical Instrumentation Engineers (SPIE) [DOI: 10.1117/1.JBO.18.6.067003]

Keywords: photoacoustic sensing; tissue characterization; thermal treatment; high-intensity focused ultrasound ablation; coagulated tissue.

Paper 12777RR received Dec. 5, 2012; revised manuscript received May 4, 2013; accepted for publication May 10, 2013; published online Jun. 3, 2013.

1 Introduction

Thermal treatments of biological tissues can benefit from non-invasive monitoring techniques to measure tissue temperature and/or tissue change (e.g., from native to coagulated) in real time to ensure safe and effective outcomes. Ultrasound imaging and magnetic resonance imaging (MRI) have been used to measure temperature and tissue changes.¹⁻⁴ However, ultrasound imaging techniques can be susceptible to problems associated with a rapid and large range of temperature variations during treatments such as in high-intensity focused ultrasound (HIFU) ablation.⁵ The low contrast between coagulated and native (nontreated) tissues in ultrasound imaging limits its ability for accurate assessment of treatment outcome, and generation of hyperechoic gas bodies during ablation does not always correspond to the coagulation extent.^{6,7} MRI, despite having good imaging contrast and high resolution,⁴ suffers from slow acquisition speed, which may limit its use in treatments with rapid tissue heating and result in extended treatment time.⁸ Moreover, the high cost and lack of portability of MRI systems are disadvantages that may restrict its widespread use for treatment monitoring.⁹

Photoacoustic (PA) imaging is an emerging technique which derives its contrast from the optical properties of the imaged object, and has been shown to be capable of providing structural, functional, and molecular information.^{10,11} Estimation of tissue

temperatures below the coagulation level may be achieved from PA signal intensity.¹²⁻¹⁵ Real-time temperature monitoring using PA techniques has been explored during photothermal¹⁶⁻¹⁸ and HIFU treatment.^{19,20} Most of these studies focused on temperature measurements, although tissue alteration during the thermal treatments which resulted in changes in tissue optical properties, also contributed to the changes in PA signals. From empirical observations, a relation between PA signal intensity and thermal dose, instead of temperature, has been suggested as a better parameter for coagulation monitoring.¹⁹ In all these studies, laser excitation at a single wavelength was employed, and to estimate temperature, a relation between PA signals and temperature was acquired in advance as a calibration.^{14,16}

Another PA method suggested for thermal treatment monitoring is based on the changes in the optical properties in thermally treated tissues. Tissues at different statuses (e.g., native or coagulated) have different compositions, resulting in different optical properties. Therefore, PA signal intensity is dependent on the tissue status. In most studies, the PA signal intensity increased during or after coagulation, presumably as a result of the increased chromophore concentration due to dehydration²¹ and/or the formation of methemoglobin (MetHb), a strong optical absorber over a broad optical spectrum.²¹⁻²³ Contradictory to the findings from most *ex vivo* studies, Chitnis et al. reported a negative contrast in HIFU lesions in the kidney of a live rat,²⁴ which was explained by the difference in the heating mechanism and the difference between *in vivo* and *ex vivo* conditions. However, no matter whether coagulated tissue exhibits a negative or positive contrast, PA signals at a single

Address all correspondence to: Xueding Wang, University of Michigan, Department of Radiology, 1301 Catherine Street, 3226B Med Sci 1, Ann Arbor, Michigan 48109. E-mail: xdwang@umich.edu, or Cheri X. Deng, University of Michigan, Department of Biomedical Engineering, 2200 Bonisteel Boulevard, Ann Arbor, Michigan 48109. Tel: +1 734-936-2855; Fax: +1 734-936-1905; E-mail: cx deng@umich.edu

wavelength cannot provide a clear indication of tissue changes in real time because the increasing temperature during thermal treatment also affects PA signals.

Considering the thermal expansion of an absorbing medium heated by a short laser pulse with incident laser fluence F_0 , we can calculate the pressure rise $\Delta P(z)$ in the irradiated volume under temporal pressure confinement by^{25,26}

$$\Delta P(z) = \left(\frac{\beta c^2}{C_p}\right) \mu_a F = \Gamma \mu_a F(z) = \Gamma \mu_a e^{-z\sqrt{3\mu_a(\mu_a+\mu_s')}} F_0, \quad (1)$$

where μ_a and μ_s' are the optical absorption coefficient and the reduced scattering coefficient, respectively, z is the depth along the photoacoustic receiving beam, and $\Gamma = \beta c^2 / C_p$ is the Grüneisen parameter with β , c , and C_p being the thermal coefficient of volume expansion, speed of sound, and heat capacity at constant pressure, respectively. Γ is both temperature and tissue type/status dependent. When the tissue status remains unchanged, Γ is often empirically assumed to be linearly related to temperature.¹⁴ However, variations in the contents of water, lipid, proteins, and other materials in different tissues yield different β , c , and C_p , and different dependencies of these parameters on temperature.^{14,27} For example, PA signal amplitude in lipid-rich plaques and lard decreases with temperature rise, which is clearly different from water-based tissues.^{28,29}

In order to resolve the problem of combined effects from tissue temperature and optical properties on PA signals during thermal treatments, we propose a dual-wavelength PA technique. The temperature-dependent Γ in Eq. (1) is removed by dividing PA signal intensities obtained at two different wavelengths at the same temperature. The resulting ratio will then depend only on the tissue optical properties; thus tissue status may be obtained without the effect of tissue temperature. In this study, we conducted experiments using water bath heating of *ex vivo* porcine myocardium tissue specimens to test our proposed dual-wavelength PA technique.

2 Materials and Methods

2.1 Dual-Wavelength PA Technique

In this study, we examined the simplest case where the PA signals were generated from locations close to tissue surface. In this case, Eq. (1) can be simplified into $\Delta P(z=0) = \Gamma \mu_a F_0$. In most former studies,^{12–16,18,20} the temperature dependency of tissue optical properties was not considered because major tissue absorbers, such as hemoglobin, have been reported to exhibit minor changes in optical absorption (<3.5%) over the temperature range of 20 to 40°C.³⁰ It was also found that, in the temperature range below coagulation threshold, the optical absorption coefficient μ_a in both human skin³¹ and canine prostate³² did not change much with increased temperature. Although in these studies negligible changes in optical absorption with temperature increase were observed only at low temperature ranges (up to 40°C) since it is not feasible to measure the optical properties at high temperatures without inducing changes in tissue composition, we assume that the temperature dependency of tissue optical properties would still be negligible through the entire temperature range (up to temperatures above coagulation threshold). On the contrary, μ_a is highly dependent on the tissue type/status. For example, thermal-induced tissue coagulation could lead to significant changes in μ_a .^{33–37} Therefore, in this work,

μ_a is expressed as a function of laser wavelength and tissue type/status. The laser-induced pressure rise can now be expressed as

$$\Delta P = \Gamma(\text{tissue status } s, \text{ temperature } T) \cdot \mu_a(\text{tissue status } s, \text{ wavelength } \lambda) F_0. \quad (2)$$

If we obtain PA signals using two different wavelengths, λ_1 and λ_2 , at the same temperature and at the same time when the tissue status is also the same, the induced pressure rise can be written as $\Delta P_{(s,T,\lambda_1)} = \Gamma_{(s,T)} \mu_{a(s,\lambda_1)} F_{0(\lambda_1)}$ and $\Delta P_{(s,T,\lambda_2)} = \Gamma_{(s,T)} \mu_{a(s,\lambda_2)} F_{0(\lambda_2)}$, at the two wavelengths, respectively. By dividing $\Delta P_{(s,T,\lambda_1)}$ by $\Delta P_{(s,T,\lambda_2)}$, we define a temperature-independent parameter or ratio k as

$$k = \frac{\Delta P_{(s,T,\lambda_1)}}{\Delta P_{(s,T,\lambda_2)}} = \frac{\Gamma_{(s,T)} \mu_{a(s,\lambda_1)} F_{0(\lambda_1)}}{\Gamma_{(s,T)} \mu_{a(s,\lambda_2)} F_{0(\lambda_2)}} = \frac{\mu_{a(s,\lambda_1)}}{\mu_{a(s,\lambda_2)}} \cdot \frac{F_{0(\lambda_1)}}{F_{0(\lambda_2)}} = \frac{\mu_{a(s,\lambda_1)}}{\mu_{a(s,\lambda_2)}} \cdot m, \quad (3)$$

where $m = F_{0(\lambda_1)} / F_{0(\lambda_2)}$ is irrelevant to the tissue and, therefore, can be assumed constant if the light fluence on the sample is stable or can be normalized by monitoring the laser output energy. Now that the temperature-dependent Γ is eliminated from the equation, the parameter k depends only on the optical properties of the tissue and should be a constant for the same tissue type/status under different temperatures. Because k may be different for different tissue types and may change when tissue alteration occurs (e.g., coagulation), it can be used to differentiate various tissues or as an indicator for thermal-induced tissue coagulation.

Upon examination of the pressure rise obtained at different temperatures, T_0 and T_1 , with corresponding tissue statuses s_0 and s_1 , we can write $\Delta P_{(s_0,T_0,\lambda)} = \Gamma_{(s_0,T_0)} \mu_{a(s_0,\lambda)} F_{0(\lambda)}$ and $\Delta P_{(s_1,T_1,\lambda)} = \Gamma_{(s_1,T_1)} \mu_{a(s_1,\lambda)} F_{0(\lambda)}$ based on Eq. (2). The relative signal change from T_0 to T_1 is therefore expressed as

$$\begin{aligned} & \frac{\Delta P_{(s_1,T_1,\lambda)} - \Delta P_{(s_0,T_0,\lambda)}}{\Delta P_{(s_0,T_0,\lambda)}} \\ &= \frac{\Gamma_{(s_1,T_1)} \mu_{a(s_1,\lambda)} F_{0(\lambda)} - \Gamma_{(s_0,T_0)} \mu_{a(s_0,\lambda)} F_{0(\lambda)}}{\Gamma_{(s_0,T_0)} \mu_{a(s_0,\lambda)} F_{0(\lambda)}} \quad (4) \\ &= \frac{\Gamma_{(s_1,T_1)} \mu_{a(s_1,\lambda)} - \Gamma_{(s_0,T_0)} \mu_{a(s_0,\lambda)}}{\Gamma_{(s_0,T_0)} \mu_{a(s_0,\lambda)}}. \end{aligned}$$

If the tissue status remains the same from T_0 to T_1 , then $s_1 = s_0$ and the relative signal change is simplified to $[\Gamma_{(s_0,T_1)} - \Gamma_{(s_0,T_0)}] / \Gamma_{(s_0,T_0)}$, which is independent of the laser wavelength. Therefore, we can expect the relative signal change to be the same for different wavelengths when there is no change in tissue type/status.

2.2 HIFU Ablation and Dual-Wavelength PA Sensing

Ex vivo porcine myocardium specimens obtained from the local abattoir were used in this study. To demonstrate the ability of dual-wavelength PA detection technique in monitoring tissue status without being affected by temperature change, one group of tissue specimens was treated with HIFU application to generate thermal lesions prior to PA measurement, while

the other group of specimens was untreated. The HIFU system consisted of an HIFU transducer (2 MHz center frequency, $F = 0.98$, Blatek Inc., State College, Pennsylvania), a delay/pulse generator (Model 565, Berkeley Nucleonics Corp., San Rafael, California), a function generator (33220A, Agilent, Santa Clara, California), and a power amplifier (325LA, ENI, Rochester, New York), as shown in Fig. 1(a). A tissue specimen (22 mm \times 22 mm \times 13 mm) was placed in a plastic holder with the front and the back sides covered by acoustically transparent membranes (Tegaderm, 3M, St. Paul, Minnesota) to prevent possible changes in hydration and concentration of chromophores in the tissue specimen when submerged in water. Each ablation was conducted using a 20 s pulsed HIFU exposure (1500 W/cm² focal intensity, 80% duty cycle, 10 Hz pulse repetition frequency), with the HIFU focus aimed near the tissue surface for visual confirmation of the ablation outcome. The HIFU transducer was moved using translation stages to generate a bigger volume of coagulated tissue.

Figure 1(b) shows the schematic experimental setup to obtain PA signals from the HIFU lesions and nontreated tissues at various temperatures. The system consisted of a temperature-controlled water bath (Precision 280, Thermo Scientific, Waltham, Massachusetts), a circulating pump (Peri-Star Pro, World Precision Instruments Inc., Sarasota, Florida), a focused imaging transducer (10 MHz center frequency, V311, Panametrics, Waltham, Massachusetts), and a laser source. Tissue temperatures were controlled using the water bath and measured with a K-type thermocouple (0.08 mm diameter, Omega Engineering, Stamford, Connecticut), which was inserted in the specimen and sampled at 20 Hz by a data acquisition system (OMB-DAQ-3000, Omega Engineering). An Nd:YAG (Brilliant B, Quantel, Bozeman, Montana) pumped optical parametric oscillator (OPO) system (Vibrant 532 I, Optronic Inc., Carlsbad, California) provided laser pulses at 700 and 800 nm wavelengths with a pulse duration of 5.5 ns and a pulse repetition rate of 10 Hz. These two wavelengths were chosen for two main reasons: (1) the output energy from the laser system is strong and stable in this range and (2) the major chromophores at these two wavelengths include oxygenated hemoglobin (HbO₂), deoxygenated hemoglobin (Hb), and MetHb, and their optical absorptions are different between 700 and 800 nm,^{38,39} which allows detection of changes in ratio k when the concentrations of these chromophores change due to thermal coagulation. The energy of the laser beam was measured using a photodiode (Model 2031, New Focus, Santa Clara, California) for later normalization. The PA signals received from the imaging transducer, which worked on the transmission mode, were first amplified by 40 dB with a preamplifier (5052PR, Panametrics) and then recorded with a 200 MHz

sampling rate on a digital oscilloscope (54380B, Agilent). In this experiment, the temperature was only increased from room temperature to 43°C to prevent any tissue alteration. For all measurements, the laser beam was centered at the lesion center and the beam size (3 mm in diameter) was smaller than the lesion cross-section. PA signals were acquired for 10 s at each wavelength at each temperature. Gross photos of the tissue specimens were taken after the experiment.

2.3 Thermal Treatments Using Water Bath Heating

To investigate the changes in signal ratio k during thermal treatments, PA sensing was performed on tissue specimens undergoing water bath heating using the same setup in Fig. 1(b). The temperature of the water tank was gradually increased from 35 to 60°C to ensure that tissue coagulation occurred during treatment. The heating rate was $0.20 \pm 0.03^\circ\text{C}/\text{min}$ from 43 to 54°C and $0.06 \pm 0.02^\circ\text{C}/\text{min}$ from 54 to 60°C. The circulating temperature-controlled system required a longer time to raise water temperature at higher temperatures, resulting in the slower heating rate above 54°C. At each temperature/time measurement point, PA signals were acquired for 10 s at each wavelength, first at 700 nm and then at 800 nm. The time interval between the start of PA signal acquisition using 700 and 800 nm illuminations was 14.11 ± 1.05 s, with the absolute difference of the average tissue temperature being $0.07 \pm 0.05^\circ\text{C}$. The small time and temperature differences and the slow heating rate allowed our assumption that changes in the tissue status or composition during signal acquisition were negligible.

2.4 Data Processing

The normalized PA amplitude was obtained by dividing the peak-to-peak PA signal amplitude [Fig. 1(c)] by the peak amplitude of the photodiode signal [Fig. 1(d)] to minimize the effect due to the fluctuation of the laser energy over time. The measured PA signals were averaged over 10 s to improve signal-to-noise ratio. We denote the averaged normalized PA amplitude as P . The ratio k (which may differ from the k in Eq. (3) by some constant) was computed using

$$k = P_{700 \text{ nm}}/P_{800 \text{ nm}}, \quad (5)$$

where $P_{700 \text{ nm}}$ and $P_{800 \text{ nm}}$ are the measurements obtained at laser wavelengths of 700 and 800 nm, respectively.

To investigate how PA signals depend on temperature and to compare different wavelengths, the relative signal change (%) of P over temperature was computed based on Eq. (4) using

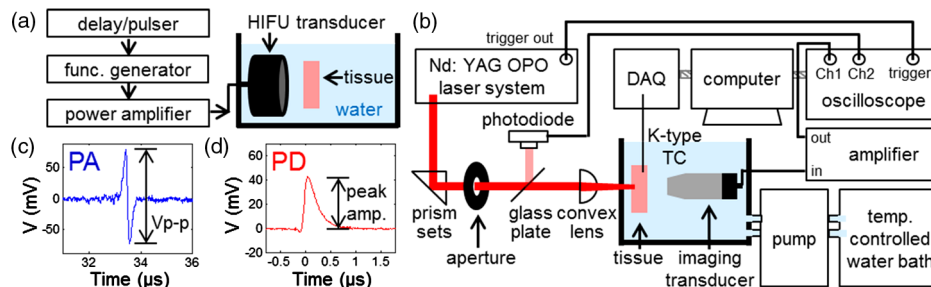


Fig. 1 Schematic illustration of experimental setup for (a) HIFU ablation and (b) PA sensing in a temperature-controlled water bath. (c) and (d) Typical PA signal and photodiode signal. Vp-p denotes the peak-to-peak amplitude.

$$\begin{aligned} &\text{Relative signal change (\%)} \text{ at temperature } T \\ &= \frac{(P_{\lambda,T} - P_{\lambda,T_0})}{P_{\lambda,T_0}} \times 100\%, \end{aligned} \quad (6)$$

where λ is 700 or 800 nm and T_0 is the reference temperature.

3 Results

3.1 Ratio k is Temperature Independent

As an example, Fig. 2(a) shows the gross photo of an HIFU lesion on the surface of a tissue specimen. As shown in Fig. 2(b) and 2(c), the mean \pm standard deviation (S.D.) of the relative signal change (%) of the averaged normalized PA amplitude P in the native (no coagulated lesion) tissues ($N = 9$) and in the HIFU lesions ($N = 8$) computed using Eq. (6) exhibits the same trend for both wavelengths used in the experiments. Since the temperature range was kept below 43°C, and measurements were made within 2 h for each sample, no tissue alteration occurred as observed from the gross photo and calculated using the thermal damage model.⁴⁰⁻⁴² Thus these results confirmed that the relative percentage change in the PA signal intensity is independent of the wavelength at any temperature when the tissue properties remain unchanged. Therefore, the ratio k between these two wavelengths is expected to be constant at different temperatures, as demonstrated in Fig. 3, where $k = P_{700 \text{ nm}}/P_{800 \text{ nm}}$ is constant from 25 to 43°C. Combining all data obtained from individual specimens and at 10 different temperatures, $k = 2.28 \pm 0.20$ in native tissues ($N = 90$) and 2.70 ± 0.18 in HIFU lesions ($N = 80$). The difference in the k value between these two groups is statistically significant (p value < 0.001). The threshold for differentiating the two groups is $k = 2.52$, as determined using the receiver-operating characteristic curve,⁴³ providing an 85.3% accuracy with an area under curve of 0.93.

3.2 Ratio k Increases with Tissue Changes During Thermal Treatment

The averaged normalized PA signal P at 700 and 800 nm from one tissue specimen subjected to water bath heating are shown in Fig. 4(a) and 4(b) to illustrate the change of PA signals with increasing temperature. Both of the PA signal amplitudes obtained with 700 and 800 nm laser excitations increased

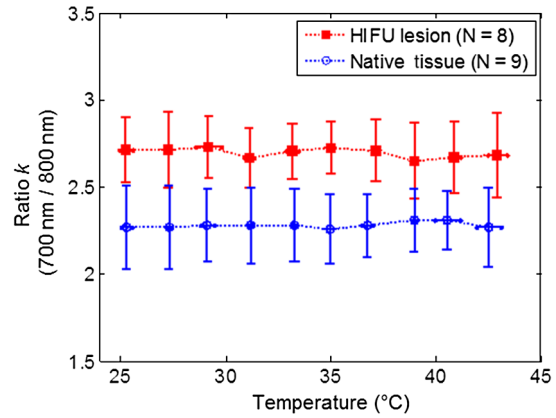


Fig. 3 Comparison of the dual-wavelength ratio k (700 nm/800 nm) in HIFU lesions and native tissues as a function of temperature.

with increasing tissue temperature, with a relatively slower increase below 50°C and a much faster increase when temperature increased further. However, from either of these single wavelength results it is difficult to determine exactly when coagulation or changes in tissue status/content occurred, as both increased temperature and tissue alteration caused the PA signals to increase in amplitude.

By taking the ratio of the PA signals from the two wavelengths to eliminate the effect of temperature in the PA signals, the change in tissue status can be better identified as shown in Fig. 4(c). Unlike P , which is temperature dependent, k is nearly constant with increasing temperature until a sharp increase appeared at 56°C, which allows clear identification of the temperature at which changes in tissue occurred.

Figure 5(a) shows the mean \pm S.D. of ratio k from five independent measurements. Again, it can be seen that k is nearly constant before it increases sharply at 55°C, suggesting that changes in the optical properties of the tissues during the coagulation process occurred at this temperature. Coagulation of the tissue samples was confirmed at the end of each experiment. Coagulated tissue appeared pinkish and white in contrast to its original dark red color. Individual curves of k for all five specimens are shown in Fig. 5(b). k in each experiment follows a similar trend, exhibiting a constant value before it increases sharply at a temperature between 55 and 58°C.

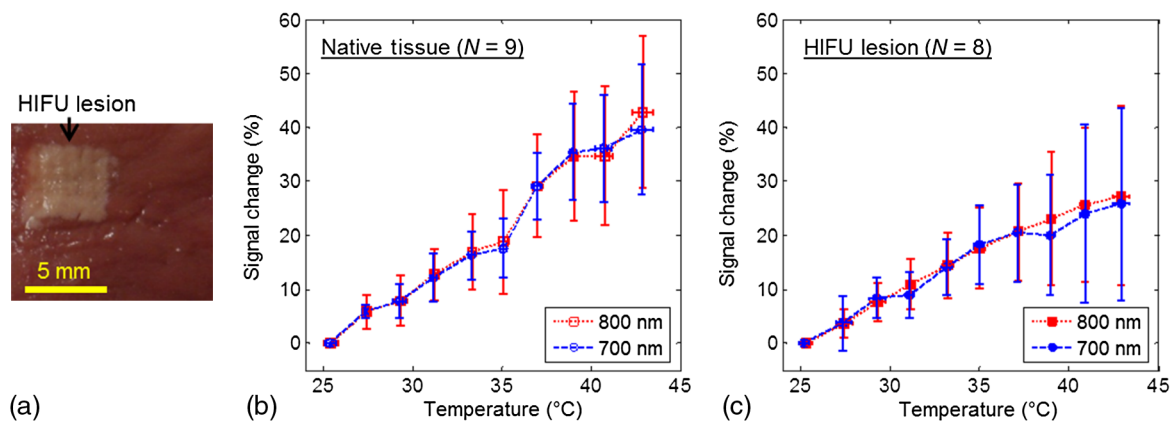


Fig. 2 (a) Gross photo of a tissue specimen with an HIFU lesion generated before PA experiment. (b) and (c) The relative signal change (%) of the averaged normalized PA amplitude P as a function of temperature in native tissues and in HIFU lesions. $T_0 = 25.3 \pm 0.3^\circ\text{C}$.

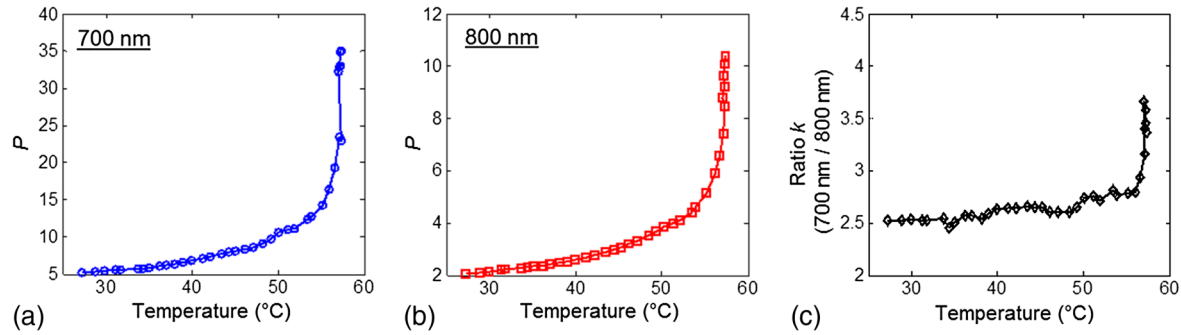


Fig. 4 An example of coagulation during water bath heating. (a) and (b) The averaged normalized PA amplitude P as a function of temperature at 700 and 800 nm wavelengths. (c) Corresponding dual-wavelength ratio k (700 nm/800 nm).

In two sets of measurements, the coagulated tissues were allowed to cool down using the temperature-controlled water bath and k values were obtained in the coagulated tissues at a lower temperature range of 37 to 44 $^{\circ}\text{C}$. Our experiments confirmed that k remained constant in this temperature range, similar to the native tissue samples, except that $k = 5.00 \pm 0.27$ in the coagulated tissues ($N = 19$), which is statistically significantly different from their native state when $k = 2.55 \pm 0.13$ ($N = 14$) with a p value < 0.001 , indicating that the tissue status alone affects the values of k .

4 Discussion

In this study, HIFU lesions were chosen as an example to illustrate the feasibility of dual-wavelength PA detection of tissue changes independent of tissue temperature because HIFU is a promising modality for noninvasive thermal ablation of tissues within a confined volume.^{9,44,45} Moreover, a system for PA-guided HIFU ablation has its advantage by using the same ultrasound transducer (either a single-element transducer⁴⁶ or an array probe⁴⁷) for both HIFU treatment and PA signal detection.

In both experiments, when tissue temperature increased with and without generating tissue alterations [Figs. 2(b), 2(c), 4(a), and 4(b)], the averaged normalized PA amplitude P increased as reported in previous studies.^{19,29,48} The relative signal change (%) in the two tissue types (i.e., with and without HIFU lesion) changes linearly with temperature (in the range of 25 to 43 $^{\circ}\text{C}$, without inducing tissue changes) for both wavelengths used, but with a different percentage change under the same temperature increment [Fig. 2(b) and 2(c)]. The reason for HIFU lesions having a smaller averaged relative percentage change is likely due to lesser water content in the coagulated tissue compared to non-treated tissues, and β and c of water have a higher and positive dependency on temperature.²⁷ The large S.D. in the relative

signal change in both tissue types may be attributed to the variations in tissue composition between different samples, leading to β and c having different dependencies on temperature.²⁷

For temperature estimation with PA sensing using a single laser wavelength, a calibration curve determining the relation between PA signal amplitude and temperature is usually required for a specific tissue type. This can be tedious and prone to error, as there are variations in the tissue composition or the proportion of each component from sample to sample. Inaccurate temperature estimations for thermal treatment monitoring can occur if a general calibration curve is used. In comparison, dual-wavelength PA sensing can directly monitor the tissue status change during thermal treatment process, as the ratio k remains constant, even with increasing temperature, until a marked increase occurs due to tissue coagulation. No calibration on the signal-temperature relationship is needed beforehand. In addition, the distinct k values for native tissues and HIFU lesions can be used for tissue characterization to detect HIFU lesions.

It is noted that k is smaller in HIFU lesions (Fig. 3) measured in our experiments compared to tissue samples coagulated by water bath heating (Fig. 5). The differences between the two heating processes (HIFU is fast and localized while water bath heating is slow and global) may lead to different tissue compositions in the coagulated tissues. Another possible reason for the higher k in tissues subjected to water bath heating is the much larger coagulated tissue volume as the coagulation occurred in the entire tissue specimen, unlike the HIFU lesions which were of much smaller dimensions (lesion depth ~ 0.5 mm). Also, ratio k of the water bath heated tissue appeared to continue to increase at the end of the heating period, suggesting that further coagulation was possible if longer and/or higher temperature heating was applied.

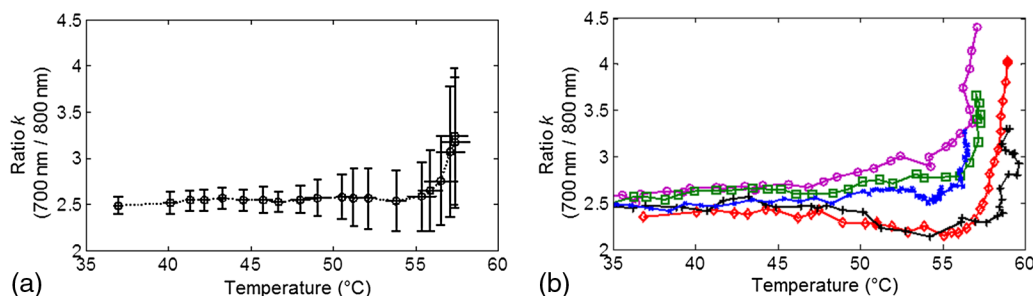


Fig. 5 Dual-wavelength ratio k (700 nm/800 nm) during the coagulation process: (a) Mean \pm S.D. ($N = 5$) and (b) individual plots as a function of temperature ($^{\circ}\text{C}$).

To choose the best wavelengths for maximum contrast or sensitivity to monitor tissue changes during thermal treatment, a complete spectrum over a broad range of wavelengths should be investigated to determine the absorption spectrum of coagulated tissues. Nilsson et al.⁴⁹ showed the absorption spectra for rat liver in the native state and laser-induced coagulated state, where μ_a , in general, increased after laser treatment for the wavelengths investigated (600 to 1050 nm), with a slightly higher increase at 700 nm compared to 800 nm. Ritz et al.⁵⁰ (400 to 2400 nm) also showed that porcine liver with water bath heating exhibited an increase in μ_a , which was greater at 700 nm compared to 800 nm. These results are compatible with our results where the ratio (700 nm/800 nm) was greater after coagulation. Since the major chromophores at 700 and 800 nm are HbO₂, Hb, and MetHb, the change in ratio k due to thermal heating most likely came from changes in proportions of hemoglobin components at high temperatures. Ideally, if we can obtain the complete spectrum over a wide range of laser wavelengths during thermal treatments in real time, any slight changes in tissue composition can be detected due to the unique absorption and scattering spectrum from each component. However, this may require a long acquisition time and, hence, may not facilitate treatment monitoring in a real-time manner. Even without the complete spectrum, we have shown here that two wavelengths are already sufficient to make distinctions between two different tissue statuses. Measurement at a wavelength with stronger water absorption may be used in the future to provide larger contrast showing dehydration as a result of thermal treatment.

The limited speed of wavelength tuning of the OPO system used in this study does not allow implementation of real-time monitoring of HIFU ablation with the dual-wavelength PA sensing technique. Our next step is to implement the technique for real-time monitoring of HIFU ablation by combining two laser systems operating at different wavelengths. Also, an ultrasound array system will be used in our future study to acquire PA images with spatiotemporal information.

5 Conclusion

We demonstrated the feasibility of a dual-wavelength PA sensing technique to detect changes in tissue optical properties due to thermal treatment. Unlike single-wavelength PA methods, our technique uses the temperature-independent ratio of the PA signals obtained at two laser wavelengths. Our method can be used to monitor tissue changes during thermal treatment without the need for a calibrated relation of PA signals and temperature in advance. Our results suggest that the technique may have the potential for monitoring thermal treatments such as those based on photothermal, radiofrequency, and HIFU ablations.

Acknowledgments

This work was supported in part by the National Institutes of Health (R01 EB008999 and R01 AR060350). The authors would also like to acknowledge Dr. Albert Shih for helpful discussions and Dr. Justin R. Rajian for assistance on the implementation of PA sensing.

References

- F. M. Fennessy and C. M. Tempny, "A review of magnetic resonance imaging-guided focused ultrasound surgery of uterine fibroids," *Top. Magn. Reson. Imag.* **17**(3), 173–179 (2006).
- A. Anand, D. Savery, and C. Hall, "Three-dimensional spatial and temporal temperature imaging in gel phantoms using backscattered ultrasound," *IEEE Trans. Ultrason. Ferroelectr. Freq. Control* **54**(1), 23–31 (2007).
- R. M. Arthur et al., "3-D in vitro estimation of temperature using the change in backscattered ultrasonic energy," *IEEE Trans. Ultrason. Ferroelectr. Freq. Control* **57**(8), 1724–1733 (2010).
- K. Hynynen, "MRI-guided focused ultrasound treatments," *Ultrasonics* **50**(2), 221–229 (2010).
- N. R. Miller, J. C. Bamber, and P. M. Meaney, "Fundamental limitations of noninvasive temperature imaging by means of ultrasound echo strain estimation," *Ultrasound Med. Biol.* **28**(10), 1319–1333 (2002).
- J. Huang, J. S. Xu, and R. X. Xu, "Heat-sensitive microbubbles for intraoperative assessment of cancer ablation margins," *Biomaterials* **31**(6), 1278–1286 (2010).
- S. N. Goldberg, G. S. Gazelle, and P. R. Mueller, "Thermal ablation therapy for focal malignancy: a unified approach to underlying principles, techniques, and diagnostic imaging guidance," *Am. J. Roentgenol.* **174**(2), 323–331 (2000).
- I. Rivens et al., "Treatment monitoring and thermometry for therapeutic focused ultrasound," *Int. J. Hyperthermia* **23**(2), 121–139 (2007).
- J. E. Kennedy, "High-intensity focused ultrasound in the treatment of solid tumours," *Nat. Rev. Cancer* **5**(4), 321–327 (2005).
- S. Mallidi, G. P. Luke, and S. Emelianov, "Photoacoustic imaging in cancer detection, diagnosis, and treatment guidance," *Trends Biotechnol.* **29**(5), 213–221 (2011).
- M. Xu and L. V. Wang, "Photoacoustic imaging in biomedicine," *Rev. Sci. Instrum.* **77**(4), 041101 (2006).
- K. V. Larin et al., "Monitoring of temperature distribution in tissues with photoacoustic technique in real time," *Proc. SPIE* **3916**, 311–321 (2000).
- R. O. Esenaliev et al., "Real-time photoacoustic monitoring of temperature in tissues," *Proc. SPIE* **3601**, 268–275 (1999).
- I. V. Larina, K. V. Larin, and R. O. Esenaliev, "Real-time photoacoustic monitoring of temperature in tissues," *J. Phys. D Appl. Phys.* **38**(15), 2633–2639 (2005).
- M. Pramanik and L. V. Wang, "Thermoacoustic and photoacoustic sensing of temperature," *J. Biomed. Opt.* **14**(5), 054024 (2009).
- J. Shah et al., "Photoacoustic imaging and temperature measurement for photothermal cancer therapy," *J. Biomed. Opt.* **13**(3), 034024 (2008).
- G. Schule et al., "Noninvasive photoacoustic temperature determination at the fundus of the eye during laser irradiation," *J. Biomed. Opt.* **9**(1), 173–179 (2004).
- S. Kim et al., "Ultrasound and photoacoustic image-guided photothermal therapy using silica-coated gold nanorods: in-vivo study," in *2010 IEEE Intl. Ultrasonics Symp.*, pp. 233–236, IEEE, New York, NY (2010).
- H. Cui and X. Yang, "Real-time monitoring of high-intensity focused ultrasound ablations with photoacoustic technique: an in vitro study," *Med. Phys.* **38**(10), 5345–5350 (2011).
- P. V. Chitnis et al., "A photoacoustic sensor for monitoring in situ temperature during HIFU exposures," in *AIP Conf. Proc.*, Vol. 1215, pp. 267–272, American Institute of Physics, New York, NY (2010).
- S. M. Nikitin, T. D. Khokhlova, and I. M. Pelivanov, "Temperature dependence of the photoacoustic transformation efficiency in ex vivo tissues for application in monitoring thermal therapies," *J. Biomed. Opt.* **17**(6), 061214 (2012).
- T. D. Khokhlova et al., "Opto-acoustic diagnostics of the thermal action of high-intensity focused ultrasound on biological tissues: the possibility of its applications and model experiments," *Quantum Electron.* **36**(12), 1097–1102 (2006).
- J. F. Black and J. K. Barton, "Chemical and structural changes in blood undergoing laser photocoagulation," *Photochem. Photobiol.* **80**(1), 89–97 (2004).
- P. V. Chitnis et al., "Feasibility of photoacoustic visualization of high-intensity focused ultrasound-induced thermal lesions in live tissue," *J. Biomed. Opt.* **15**(2), 021313 (2010).
- A. A. Oraevsky, S. L. Jacques, and F. K. Tittel, "Measurement of tissue optical properties by time-resolved detection of laser-induced transient stress," *Appl. Opt.* **36**(1), 402–415 (1997).
- V. E. Gusev and A. A. Karabutov, *Laser Photoacoustics*, American Institute of Physics, New York (1993).

27. F. A. Duck, *Physical Properties of Tissue*, Academic Press Inc., San Diego, CA (1990).
28. B. Wang and S. Emelianov, "Thermal intravascular photoacoustic imaging," *Biomed. Opt. Express* **2**(11), 3072–3078 (2011).
29. S. M. Nikitin, T. D. Khokhlova, and I. M. Pelivanov, "In-vitro study of the temperature dependence of the optoacoustic conversion efficiency in biological tissues," *Quantum Electron.* **42**(3), 269–276 (2012).
30. R. Sfameni et al., "Near infrared absorption spectra of human deoxy- and oxyhaemoglobin in the temperature range 20–40 degrees C," *Biochem. Biophys. Acta* **1340**(2), 165–169 (1997).
31. J. Laufer et al., "Effect of temperature on the optical properties of ex vivo human dermis and subdermis," *Phys. Med. Biol.* **43**(9), 2479–2489 (1998).
32. W. H. Nau, R. J. Roselli, and D. F. Milam, "Measurement of thermal effects on the optical properties of prostate tissue at wavelengths of 1,064 and 633 nm," *Lasers Surg. Med.* **24**(1), 38–47 (1999).
33. J. P. Ritz et al., "Optical properties of native and coagulated porcine liver tissue between 400 and 2400 nm," *Lasers Surg. Med.* **29**(3), 205–212 (2001).
34. H. Ao et al., "Thermal coagulation-induced changes of the optical properties of normal and adenomatous human colon tissues in vitro in the spectral range 400–1,100 nm," *Phys. Med. Biol.* **53**(8), 2197–2206 (2008).
35. J. W. Pickering et al., "Changes in the optical properties (at 632.8 nm) of slowly heated myocardium," *Appl. Opt.* **32**(4), 367–371 (1993).
36. J. W. Pickering, P. Posthumus, and M. J. van Gemert, "Continuous measurement of the heat-induced changes in the optical properties (at 1,064 nm) of rat liver," *Lasers Surg. Med.* **15**(2), 200–205 (1994).
37. M. G. Skinner et al., "Changes in optical properties of ex vivo rat prostate due to heating," *Phys. Med. Biol.* **45**(5), 1375–1386 (2000).
38. T. Vo-Dinh, ed., *Biomedical Photonics Handbook*, CRC Press, Boca Raton, FL (2003).
39. L. L. Randeberg et al., "Methemoglobin formation during laser induced photothermolysis of vascular skin lesions," *Lasers Surg. Med.* **34**(5), 414–419 (2004).
40. S. A. Sapareto and W. C. Dewey, "Thermal dose determination in cancer-therapy," *Int. J. Radiat. Oncol.* **10**(6), 787–800 (1984).
41. D. Haemmerich, J. G. Webster, and D. M. Mahvi, "Thermal dose versus isotherm as lesion boundary estimator for cardiac and hepatic radio-frequency ablation," in *Proc. 25th Annual Intl. Conf. IEEE Engineering in Medicine and Biology Society*, pp. 134–137, IEEE, New York, NY (2003).
42. P. S. Yarmolenko et al., "Thresholds for thermal damage to normal tissues: an update," *Int. J. Hyperthermia* **27**(4), 320–343 (2011).
43. C. E. Metz, "Basic principles of ROC analysis," *Semin. Nucl. Med.* **8**(4), 283–298 (1978).
44. G. ter Haar, "Harnessing the interaction of ultrasound with tissue for therapeutic benefit: high-intensity focused ultrasound," *Ultrasound Obst. Gyn.* **32**(5), 601–604 (2008).
45. S. Crouzet et al., "High intensity focused ultrasound (HIFU) for prostate cancer: current clinical status, outcomes and future perspectives," *Int. J. Hyperthermia* **26**(8), 796–803 (2010).
46. H. Cui, J. Staley, and X. Yang, "Integration of photoacoustic imaging and high-intensity focused ultrasound," *J. Biomed. Opt.* **15**(2), 021312 (2010).
47. A. Prost et al., "Photoacoustic-guided ultrasound therapy with a dual-mode ultrasound array," *J. Biomed. Opt.* **17**(6), 061205 (2012).
48. K. V. Larin, I. V. Larina, and R. O. Esenaliev, "Monitoring of tissue coagulation during thermotherapy using optoacoustic technique," *J. Phys. D Appl. Phys.* **38**(15), 2645–2653 (2005).
49. A. M. K. Nilsson et al., "Changes in spectral shape of tissue optical properties in conjunction with laser-induced thermotherapy," *Appl. Opt.* **37**(7), 1256–1267 (1998).
50. J. P. Ritz et al., "Optical properties of native and coagulated porcine liver tissue between 400 and 2400 nm," *Lasers Surg. Med.* **29**(3), 205–212 (2001).